Dynamic scaling in the vicinity of the Luttinger liquid fixed point

2002 J. Phys.: Condens. Matter 14 8513

(http://iopscience.iop.org/0953-8984/14/36/309)

INSTITUTE OF PHYSICS PUBLISHING JOURNAL OF PHYSICS: CONDENSED MATTER

J. Phys.: Condens. Matter **14** (2002) 8513–8535 PII: S0953-8984(02)35728-X

Dynamic scaling in the vicinity of the Luttinger liquid fixed point

Tom Busche, Lorenz Bartosch and Peter Kopietz

Institut für Theoretische Physik, Universität Frankfurt, Robert-Mayer-Strasse 8, 60054 Frankfurt, Germany

Received 10 April 2002, in final form 10 July 2002
Published 29 August 2002
Online at stacks.iop.org/JPhysCM/14/8513

Abstract

We calculate the single-particle spectral function $A(k, \omega)$ of a one-dimensional Luttinger liquid by means of a functional renormalization group (RG) approach. Given an infrared energy cut-off $\Lambda = \Lambda_0 e^{-l}$, our approach yields the spectral function in the scaling form, $A_\Lambda(k_F + p, \omega) = \tau Z_l \tilde{A}_l(p\xi, \omega\tau)$, where k_F is the Fermi momentum, Z_l is the wavefunction renormalization factor, $\tau = 1/\Lambda$ is the timescale and $\xi = v_F/\Lambda$ is the length scale associated with Λ. At the Luttinger liquid fixed point ($l \to \infty$) our RG result for $A(k, \omega)$ exhibits the correct anomalous scaling properties, and for $k = \pm k_F$ agrees exactly with the well known bosonization result at weak coupling. Our calculation demonstrates that the field rescaling is essential for obtaining the crossover from Fermi liquid behaviour to Luttinger liquid behaviour from a truncation of the hierarchy of exact RG flow equations as the infrared cut-off Λ is reduced.

1. Introduction

For many years the renormalization group (RG) has been used to study interacting Fermi systems in one spatial dimension [1]. The success of RG methods in one dimension relies on the fact that at low energies, the two-body interactions between fermions can be parametrized in terms of four coupling constants, which are usually called g_1 (backward scattering), g_2 (forward scattering of fermions propagating in opposite directions), g_3 (Umklapp scattering) and g_4 (forward scattering of fermions propagating in the same direction). Most authors have focused on the calculation of the RG β-functions, which in the Wilsonian RG [2–5] describe the flow of these couplings as the degrees of freedom are eliminated and rescaled[1]. However, the RG β-functions do not completely describe the physical behaviour of the system. In particular, the RG β-functions do not contain information about the single-particle excitations.

[1] Note that in [1] the RG β-functions are derived by means of the field theory version of the RG, which relies on the renormalizability of the model.

To investigate these, one should calculate the momentum- and frequency-dependent single-particle spectral function $A(k, \omega)$, which at temperature $T = 0$ is related to the imaginary part of the single-particle Green function $G(k, \omega)$ via

$$A(k, \omega) = -\frac{1}{\pi}\mathrm{Im}\, G(k, \omega + \mathrm{i}0). \tag{1.1}$$

In the absence of backward and Umklapp scattering, the leading asymptotic long-distance and long-time behaviour of the single-particle Green function $G(x, t)$ in the spacetime domain can be calculated via bosonization if the energy dispersion is linearized around the Fermi points (Tomonaga–Luttinger model, TLM) [6, 7]. Obviously, in order to obtain the spectral function, one should calculate the Fourier transform $G(k, \omega)$ of $G(x, t)$, which in general cannot be done exactly. For the spinless TLM with g_2-interactions, which we will consider in this work, a mathematically non-rigorous but physically reasonable asymptotic analysis yields at temperature $T = 0$, for wavevectors close to $\pm k_F$ and for low energies [8–11],

$$A_{TL}(\pm(k_F + p), \omega) \approx \Lambda_0^{-\eta}\frac{\eta}{2}\Theta(\omega^2 - (v_c p)^2)|\omega - v_c p|^{-1+\eta/2}|\omega + v_c p|^{\eta/2}, \tag{1.2}$$

where Λ_0 is some ultraviolet cut-off with units of energy (for example a band width cut-off). At weak coupling the anomalous dimension η and the velocity v_c of collective charge excitations are to leading order

$$\eta \approx \frac{\tilde{g}^2}{8}, \tag{1.3}$$

$$v_c \approx v_F\left(1 - \frac{\tilde{g}^2}{8}\right). \tag{1.4}$$

Here v_F is the bare Fermi velocity and

$$\tilde{g} = g_2/(\pi v_F) \tag{1.5}$$

is the dimensionless coupling describing forward scattering of electrons propagating in different directions. Equation (1.2) satisfies a simple scaling law: for an *arbitrary* length ξ we may write

$$A_{TL}(\pm(k_F + p), \omega) = \tau\left(\frac{\xi_0}{\xi}\right)^{\eta}\tilde{A}_{\mathrm{TL}}(p\xi, \omega\tau), \tag{1.6}$$

where $\tau = \xi/v_F$ is the timescale associated with ξ, and the length $\xi_0 = v_F/\Lambda_0$ corresponds to the ultraviolet cut-off Λ_0. The dimensionless scaling function $\tilde{A}_{TL}(q, \epsilon)$ is

$$\tilde{A}_{TL}(q, \epsilon) = \frac{\eta}{2}\Theta(\epsilon^2 - (\tilde{v}q)^2)|\epsilon - \tilde{v}q|^{-1+\eta/2}|\epsilon + \tilde{v}q|^{\eta/2}, \tag{1.7}$$

where q and ϵ are dimensionless variables, and $\tilde{v} = v_c/v_F$ is the dimensionless velocity renormalization factor. The dynamic exponent (defined via $\tau \propto \xi^z$) is in this case given by $z = 1$. The dynamic scaling function (1.7) is scale invariant, so that for an arbitrary scale factor s

$$\tilde{A}_{TL}(sq, s\epsilon) = s^{-1+\eta}\tilde{A}_{TL}(q, \epsilon). \tag{1.8}$$

This scale invariance is a consequence of the fact that the TLM represents a critical system, corresponding to the Luttinger liquid fixed point [12]. Hence, the RG β-function of the TLM vanishes identically. It is generally accepted that the TLM describes the generic low-energy and long-wavelength properties of one-dimensional Fermi systems with dominant forward scattering. Thus, the TLM is an effective model which in the regime where backward and Umklapp scattering are irrelevant emerges at low energies when the high-energy degrees of freedom are integrated out in a Wilsonian RG.

In the theory of dynamic critical phenomena [13, 14] it is usually assumed that correlation functions close to the critical point can be written in the dynamic scaling form (1.6), with some dynamic scaling function $\tilde{A}(p\xi, \omega\tau)$. The dynamic scaling function depends on ξ only implicitly via $p\xi$ and $\omega\tau = \omega\xi/v_F$. For example, at finite temperatures, where we may identify $\xi = v_F/T$ and $\tau \approx 1/T$, the scaling function $\tilde{A}_{TL}(p\xi, \omega\tau)$ of the TLM has been discussed by Orgad, Kivelson and collaborators [15].

Suppose now that we iterate the RG to some large scale factor $l = \ln(\Lambda_0/\Lambda)$, and write the resulting spectral function in the scaling form analogous to equation (1.6),

$$A_\Lambda(k_F + p, \omega) = \tau\left(\frac{\xi_0}{\xi}\right)^\eta \tilde{A}_l(p\xi, \omega\tau). \tag{1.9}$$

According to the above argument, we would expect that for large l the scaling function $\tilde{A}_l(q, \epsilon)$ becomes independent of l and approaches $\tilde{A}_{TL}(q, \epsilon)$ for large $|q|$ and $|\epsilon|$. In this work we shall show that this is only true if the limit $l \to \infty$ may be taken. If there is a finite physical infrared cut-off, the flow of l has to be stopped at a finite scale l_*. Under such circumstances there exists another physical limiting procedure where $|q|$ and $|\epsilon|$ are large compared with unity, but the difference $|\epsilon| - \tilde{v}|q|$ remains small. In this regime we find that $\tilde{A}_{l_*}(q, \epsilon)$ behaves completely differently from the scaling function of the TLM.

We shall here attempt to calculate the spectral function of the spinless g_2-TLM using RG methods. Therefore we shall calculate the RG flow of the irreducible *two-point* vertex. Recall that the usual RG β-function describes the flow of the momentum- and frequency-independent part of the irreducible *four-point* vertex. Surprisingly, the problem of calculating the spectral function of a strongly correlated fermionic system like the TLM via RG methods has not received much attention. In fact, with the exception of the recent work by Ferraz [16], where the spectral function of a special two-dimensional Fermi system has been calculated by means of the field theory RG, we are not aware of any RG calculation of the spectral line shape of a strongly correlated fermionic many-body system. Note that in order to obtain a non-trivial k- and ω-dependence and the anomalous scaling properties given in equation (1.6), one should retain infinitely many couplings which are irrelevant by naive power counting. In other words, one needs to keep track of the RG flow of coupling functions. At the first sight, this seems to be a formidable task, which is impossible to carry out in practice. Nevertheless, in this work we shall show that at weak coupling a simple truncation of the hierarchy of functional RG equations for the irreducible vertex functions yields an expression for the spectral function which has the correct anomalous scaling properties and, at least for $k = \pm k_F$, agrees with the exact result known from bosonization.

2. Exact flow equations

Originally, exact RG flow equations were developed in field theory and statistical physics to study systems in the vicinity of a critical point [17–22]. Recently, several authors have started to apply these methods to interacting Fermi systems at finite densities [23–26]. In the normal state the existence of a Fermi surface adds some new complexity to the problem: because the single-particle Green function exhibits singularities on the entire Fermi surface, the Fermi surface plays the role of a continuum (in $d > 1$) of RG fixed points. However, this fixed point manifold is not known *a priori*, and should be calculated self-consistently within the RG. In [27] we have shown how the true Fermi surface of the interacting system can be calculated from the requirement that the RG approaches a fixed point. Fortunately, in one dimension we know *a priori* that the Fermi surface (which consists of two points $\pm k_F$) is not renormalized by

the interactions [28], so that the above-mentioned problem of a self-consistent determination of the Fermi surface does not arise.

2.1. Definition of the model and notations

The starting point of our calculation is the exact flow equations derived in [27], which give the RG flow of the one-particle irreducible vertices when degrees of freedom are integrated out and a subsequent rescaling step is applied. For convenience we shall now briefly present these equations for the special case of one dimension, using a slightly different notation than in [27]. We shall work at zero temperature, but expect that our results also describe temperatures $T > 0$ as long as we consider energy scales large compared with T. In one dimension, the Fermi surface consists of two points, αk_F, where $\alpha = \pm 1$ labels the right and left Fermi points. An arbitrary wavevector k can be written as

$$k = \alpha(k_F + p), \tag{2.1}$$

where $\alpha = +1$ for $k > 0$ and -1 for $k < 0$. Note that the deviation $p = \alpha(k - \alpha k_F)$ from $\pm k_F$ is always measured locally outwards, which is different from the convention usually adopted in bosonization [1, 6, 7, 12]. For small p we may expand the non-interacting energy dispersion ϵ_k around the Fermi points,

$$\epsilon_{\alpha(k_F+p)} = \epsilon_{k_F} + v_F p + \frac{p^2}{2m} + \cdots. \tag{2.2}$$

Here v_F is the Fermi velocity and m is the mass of the non-interacting fermions. As discussed in [27], the expansion (2.2) is around the true Fermi momentum of the interacting many-body system. Of course, in one dimension the interacting and non-interacting k_F are identical if we compare systems with the same density. Note that by time reversal invariance $\epsilon_k = \epsilon_{-k}$, so that v_F and m are independent of α. For $|p| \ll k_F$ it is reasonable to linearize the energy dispersion and neglect the term of order p^2 in equation (2.2). Introducing an infrared band-width cut-off Λ and an ultraviolet cut-off Λ_0 with units of energy, the non-interacting Matsubara Green function is

$$G^0_{\Lambda,\Lambda_0}(\alpha(k_F + p), \mathrm{i}\omega) = \frac{\Theta(\Lambda_0 > v_F|p| > \Lambda)}{\mathrm{i}\omega - v_F p}, \tag{2.3}$$

where $\mathrm{i}\omega$ is a fermionic Matsubara frequency, and

$$\Theta(x_2 > x > x_1) = \Theta(x_2 - x) - \Theta(x_1 - x) = \begin{cases} 1 & \text{if } x_2 > x > x_1 \\ 0 & \text{else.} \end{cases} \tag{2.4}$$

Later we shall also write

$$\Theta(x_2 > x_1) = \Theta(x_2 - x_1) = \begin{cases} 1 & \text{if } x_2 > x_1 \\ 0 & \text{else.} \end{cases} \tag{2.5}$$

Taking the limit $\Lambda_0 \to \infty$ in equation (2.3) amounts to extending the linear energy dispersion on both branches from $-\infty$ to $+\infty$. The unphysical states with energies far below the Fermi energy introduced in this way are occupied according to the Pauli principle. It is generally accepted that this filled Dirac sea is dynamically irrelevant and does not modify the low-energy physics. However, the precise way in which the cut-off is removed can affect the numerical value of the various Luttinger liquid parameters [29]. At this point we shall keep Λ_0 finite and assume that the bare electron–electron interaction of the model is characterized by a momentum- and frequency-independent totally antisymmetric irreducible four-point vertex of the form

$$\Gamma^{(4)}_{\Lambda_0}(K_1', K_2'; K_2, K_1) = A_{\alpha_1'\alpha_2';\alpha_2\alpha_1} g_0, \tag{2.6}$$

where $K = (k, \mathrm{i}\omega) = (\alpha(k_F + p), \mathrm{i}\omega)$ and

$$A_{\alpha_1'\alpha_2';\alpha_2\alpha_1} = \delta_{\alpha_1',\alpha_1}\delta_{\alpha_2',\alpha_2} - \delta_{\alpha_2',\alpha_1}\delta_{\alpha_1',\alpha_2} = D_{\alpha_1'\alpha_2';\alpha_2\alpha_1} - E_{\alpha_1'\alpha_2';\alpha_2\alpha_1} \tag{2.7}$$

is antisymmetric with respect to the exchange $\alpha_1 \leftrightarrow \alpha_2$ or $\alpha_1' \leftrightarrow \alpha_2'$. For later convenience we have introduced the notations

$$D_{\alpha_1'\alpha_2';\alpha_2\alpha_1} = \delta_{\alpha_1',\alpha_1}\delta_{\alpha_2',\alpha_2} \qquad \text{(direct term)} \tag{2.8}$$

$$E_{\alpha_1'\alpha_2';\alpha_2\alpha_1} = \delta_{\alpha_2',\alpha_1}\delta_{\alpha_1',\alpha_2} \qquad \text{(exchange term)}. \tag{2.9}$$

Note that due to this antisymmetrization g_4-processes do not appear in the initial action. In the limits $\Lambda_0 \to \infty$ and $\Lambda \to 0$ the Green function of the model defined by equations (2.3) and (2.6) can be calculated exactly in the spacetime domain via bosonization. The generally accepted result for the spectral function is given in equation[2] (1.2).

2.2. *Scaling functions and flow equations*

For the explicit RG-calculations we use the infrared energy-band cut-off

$$\Lambda = \Lambda_0 \mathrm{e}^{-l}, \tag{2.10}$$

and follow the flow of the correlation functions as the logarithmic flow parameter l increases. The energy scale Λ is related to the length scale ξ and the timescale τ defined below equation (1.6) via

$$\xi = v_F\tau = v_F/\Lambda. \tag{2.11}$$

From these quantities, we may construct dimensionless scaling variables[3],

$$q = p\xi = (\alpha k - k_F)v_F/\Lambda, \qquad \epsilon = \omega\tau = \omega/\Lambda, \tag{2.12}$$

and write the exact single-particle Matsubara Green function of the theory with infrared cut-off Λ and ultraviolet cut-off Λ_0 in the dynamic scaling form [13, 14]

$$G_{\Lambda,\Lambda_0}(k, \mathrm{i}\omega) = \tau Z_l \tilde{G}_l(p\xi, \mathrm{i}\omega\tau), \tag{2.13}$$

where $\tilde{G}_l(q, \mathrm{i}\epsilon)$ is a dimensionless dynamic scaling function. Here the wavefunction renormalization factor Z_l is related to the irreducible self-energy $\Sigma_\Lambda(k, \mathrm{i}\omega)$ as usual,

$$Z_l = \frac{1}{1 - \frac{\partial\Sigma_\Lambda(k_F, \mathrm{i}\omega)}{\partial(\mathrm{i}\omega)}|_{\omega=0}}. \tag{2.14}$$

Note that by time-reversal symmetry Z_l and Σ_Λ are independent of α. It is also convenient to set

$$\tilde{G}_l(q, \mathrm{i}\epsilon) = \frac{\Theta(\mathrm{e}^l > |q| > 1)}{r_l(q, \mathrm{i}\epsilon)}, \tag{2.15}$$

where

$$r_l(q, \mathrm{i}\epsilon) = Z_l[\mathrm{i}\epsilon - q] + \tilde{\Gamma}_l^{(2)}(q, \mathrm{i}\epsilon), \tag{2.16}$$

and

$$\tilde{\Gamma}_l^{(2)}(q, \mathrm{i}\epsilon) = -\Lambda^{-1}Z_l[\Sigma_\Lambda(k_F + q\Lambda/v_F, \mathrm{i}\epsilon\Lambda) - \Sigma(k_F, \mathrm{i}0)]. \tag{2.17}$$

Here $\Sigma(k, \mathrm{i}\omega) = \lim_{\Lambda\to 0}\Sigma_\Lambda(k, \mathrm{i}\omega)$ is the exact self-energy of the model without infrared cut-off. As we will see later, equation (2.17) generally approaches a non-zero value even

[2] Note that the parameter g_2 of the TLM should not be confused with g_0 given in equation (2.6); the precise relation between these couplings will become evident in section 4, equation (4.4).

[3] We are using here a different notation than in our previous work [27]: ξ of [27] is now called Λ, whereas ξ is now a length, as is customary in the theory of critical phenomena.

for $q = \epsilon = 0$ and $\Lambda \to 0$. Following [27], we also define the scaling functions for the higher-order irreducible vertices,

$$\tilde{\Gamma}_l^{(2n)}(Q_1', \ldots, Q_n'; Q_n, \ldots, Q_1) = \nu_0^{n-1} \Lambda^{n-2} Z_l^n \Gamma_\Lambda^{(2n)}(K_1', \ldots, K_n'; K_n, \ldots, K_1), \tag{2.18}$$

where $\Gamma_\Lambda^{(2n)}(K_1', \ldots, K_n'; K_n, \ldots, K_1)$ are the usual one-particle irreducible $2n$-point vertices, $\nu_0 = (\pi v_F)^{-1}$ is the density of states of non-interacting spinless fermions in one dimension and $K = (k, \mathrm{i}\omega)$ and $Q = (\alpha, q, \mathrm{i}\epsilon)$ are composite labels.

The rescaled irreducible two-point vertex defined in equation (2.17) satisfies the following exact flow equation [27]:

$$\partial_l \tilde{\Gamma}_l^{(2)}(Q) = (1 - \eta_l - Q\partial_Q)\tilde{\Gamma}_l^{(2)}(Q) + \dot{\Gamma}_l^{(2)}(Q), \tag{2.19}$$

where

$$\dot{\Gamma}_l^{(2)}(Q) = -\int_{Q'} \dot{G}_l(Q')\, \tilde{\Gamma}_l^{(4)}(Q, Q'; Q', Q), \tag{2.20}$$

and η_l is the flowing anomalous dimension,

$$\eta_l = -\partial_l \ln Z_l = -\frac{\partial_l Z_l}{Z_l}. \tag{2.21}$$

We have introduced the notations

$$Q\partial_Q = q\partial_q + \epsilon\partial_\epsilon, \tag{2.22}$$

$$\dot{G}_l(Q) = \frac{\delta(|q| - 1)}{r_l(Q)}, \tag{2.23}$$

$$\int_Q = \frac{1}{2} \sum_\alpha \int \mathrm{d}q \int \frac{\mathrm{d}\epsilon}{2\pi}. \tag{2.24}$$

Equation (2.19) is equivalent with the following integral equation:

$$\tilde{\Gamma}_l^{(2)}(Q) = \tilde{\Gamma}_{l=0}^{(2)}(\mathrm{e}^{-l}Q)\mathrm{e}^{(1-\bar{\eta}_l(l))l} + \int_0^l \mathrm{d}t\, \mathrm{e}^{(1-\bar{\eta}_l(t))t} \dot{\Gamma}_{l-t}^{(2)}(\mathrm{e}^{-t}Q), \tag{2.25}$$

where $\mathrm{e}^{-t}Q = (\alpha, \mathrm{e}^{-t}q, \mathrm{e}^{-t}\mathrm{i}\epsilon)$, and we have defined an averaged anomalous dimension by

$$\bar{\eta}_l(t) = \frac{1}{t} \int_0^t \mathrm{d}t'\, \eta_{l-t+t'}. \tag{2.26}$$

The flow of the inhomogeneity $\dot{\Gamma}_l^{(2)}(Q)$ on the right-hand side of equation (2.19) is controlled by the scaling function of the four-point vertex $\tilde{\Gamma}_l^{(4)}$, which satisfies the exact flow equation

$$\begin{aligned}\partial_l \tilde{\Gamma}_l^{(4)}(Q_1', Q_2'; Q_2, Q_1) = &-\left[2\eta_l + \sum_{i=1}^{2}(Q_i'\partial_{Q_i'} + Q_i\partial_{Q_i})\right]\tilde{\Gamma}_l^{(4)}(Q_1', Q_2'; Q_2, Q_1) \\ &+ \dot{\Gamma}_l^{(4)}(Q_1', Q_2'; Q_2, Q_1),\end{aligned} \tag{2.27}$$

where

$$\begin{aligned}\dot{\Gamma}_l^{(4)}(Q_1', Q_2'; Q_2, Q_1) = &-\int_Q \dot{G}_l(Q)\tilde{\Gamma}_l^{(6)}(Q_1', Q_2', Q; Q, Q_2, Q_1) \\ &- \int_Q [\dot{G}_l(Q)\tilde{G}_l(Q') + \tilde{G}_l(Q)\dot{G}_l(Q')] \\ &\times \{\tfrac{1}{2}[\tilde{\Gamma}_l^{(4)}(Q_1', Q_2'; Q', Q)\tilde{\Gamma}_l^{(4)}(Q, Q'; Q_2, Q_1)]_{K'=K_1+K_2-K} \\ &- [\tilde{\Gamma}_l^{(4)}(Q_1', Q'; Q, Q_1)\tilde{\Gamma}_l^{(4)}(Q_2', Q; Q', Q_2)]_{K'=K+K_1-K_1'} \\ &+ [\tilde{\Gamma}_l^{(4)}(Q_2', Q'; Q, Q_1)\tilde{\Gamma}_l^{(4)}(Q_1', Q; Q', Q_2)]_{K'=K+K_1-K_2'}\}.\end{aligned} \tag{2.28}$$

Here $\tilde{\Gamma}_l^{(6)}$ is the dimensionless irreducible six-point vertex. As equation (2.20) can be converted into (2.25), equation (2.27) can be transformed into the integral equation

$$\tilde{\Gamma}_l^{(4)}(Q_1', Q_2'; Q_2, Q_1) = \tilde{\Gamma}_{l=0}^{(4)}(\mathrm{e}^{-l}Q_1', \mathrm{e}^{-l}Q_2'; \mathrm{e}^{-l}Q_2, \mathrm{e}^{-l}Q_1)\mathrm{e}^{-2l\tilde{\eta}_l(l)} + \int_0^l \mathrm{d}t\, \mathrm{e}^{-2t\tilde{\eta}_l(t)}\dot{\Gamma}_{l-t}^{(4)}(\mathrm{e}^{-t}Q_1', \mathrm{e}^{-t}Q_2'; \mathrm{e}^{-t}Q_2, \mathrm{e}^{-t}Q_1). \tag{2.29}$$

2.3. Classification of couplings in the hydrodynamic regime

The above functional RG equations determine the RG flow of the momentum- and frequency-dependent irreducible vertices $\tilde{\Gamma}_l^{(2n)}(Q_1', \ldots, Q_n'; Q_n, \ldots, Q_1)$. By expanding these vertices in powers of the dimensionless scaling variables $q_i = p_i\xi$ and $\epsilon_i = \omega_i\tau$, we obtain the RG flow of the coupling constants of the model, which are the coefficients in this multi-dimensional Taylor expansion. Following the usual terminology, couplings with positive scaling dimension are called relevant, couplings with vanishing scaling dimension are called marginal and couplings with negative scaling dimension are called irrelevant. The irrelevant couplings grow at short distances (i.e. in the *ultraviolet*) and spoil the renormalizability of the theory. In this case the usual field theory RG is not applicable. On the other hand, in a Wilsonian RG the irrelevant couplings can be treated on the same footing as the relevant ones. For this reason the Wilsonian RG is very popular in condensed matter physics, where one usually has a physical ultraviolet cut-off and renormalizability is not necessary.

What is the regime of validity of the above expansion? Obviously, the expansion of the rescaled vertex functions to some finite order in powers of the dimensionless scaling variables $q_i = p_i\xi$ and $\epsilon_i = \omega_i\tau$ can be justified if these variables are small compared with unity. As long as the infrared cut-off $\Lambda = v_F/\xi = 1/\tau$ is finite, this condition can be satisfied for sufficiently small wavevectors and frequencies. If we identify ξ with the correlation length and τ with the corresponding characteristic timescale, then the expansion of $\tilde{\Gamma}_l^{(2n)}(Q_1', \ldots, Q_n'; Q_n, \ldots, Q_1)$ in powers of the scaling variables $q_i = p_i\xi$ and $\epsilon_i = \omega_i\tau$ can be viewed as an expansion of the dynamic scaling functions in the *hydrodynamic regime*, where one is interested in length scales larger than ξ and timescales longer than τ. Of course, a normal metal at zero temperature is a critical system, where ξ and τ diverge. Close to this critical state (where ξ and τ are large but finite), we expect that the correlation functions assume some scaling form. This corresponds to the *critical regime* (also called the *scaling regime*). For example, we may describe a normal metal at finite temperature in terms of flow equations derived for $T = 0$ if we stop scaling the flow equations at a finite length scale of the order of $\xi \approx v_F/T$.

For certain systems it may happen that the couplings defined in the hydrodynamic regime smoothly evolve into analogous couplings in the scaling regime, where both q_i and ϵ_i are large. This is the essence of the dynamic scaling hypothesis [13]. For example, for a Fermi liquid we expect that such a smooth crossover between the hydrodynamic and the scaling regime indeed exists, because by definition the self-energy is analytic and hence can be expanded in powers of momenta and frequencies. On the other hand, the two-point function of a Luttinger liquid is known to exhibit algebraic singularities, so that there cannot be a smooth connection between the hydrodynamic and the critical regime. In this case one expects the analytic properties of the dynamic scaling function $\tilde{\Gamma}_l^{(2)}(q, \mathrm{i}\epsilon)$ to change as we move from the hydrodynamic into the scaling regime. In this work we shall show that this is indeed the case and give an approximate expression for the scaling function.

Let us now classify the couplings according to their relevance in the hydrodynamic regime. First of all, the momentum- and frequency-independent part of the two-point vertex,

$$\tilde{\mu}_l = \tilde{\Gamma}_l^{(2)}(0), \tag{2.30}$$

is relevant. Here $\tilde{\Gamma}_l^{(2)}(0)$ stands for $\tilde{\Gamma}_l^{(2)}(\alpha, q = 0, \mathrm{i}\epsilon = \mathrm{i}0)$. From equation (2.19) it is easy to see that $\tilde{\mu}_l$ satisfies the exact flow equation

$$\partial_l \tilde{\mu}_l = (1 - \eta_l)\tilde{\mu}_l + \dot{\Gamma}_l^{(2)}(0). \tag{2.31}$$

In general we have to fine-tune the other couplings such that the relevant coupling $\tilde{\mu}_l$ approaches a fixed point. The fixed point value of $\tilde{\mu}_l$ for $l \to \infty$ is then determined by

$$(1 - \eta_\infty)\tilde{\mu}_\infty = -\dot{\Gamma}_\infty^{(2)}(0). \tag{2.32}$$

Because $\dot{\Gamma}_\infty^{(2)}(0)$ implicitly depends on $\tilde{\mu}_\infty$, equation (2.32) is really a self-consistency equation for the fixed point value of $\tilde{\mu}_l$.

There are two marginal couplings associated with the irreducible two-point vertex $\tilde{\Gamma}_l^{(2)}(Q)$: the wavefunction renormalization factor Z_l, and the Fermi velocity renormalization factor $\tilde{v}_l$. Using the definition (2.14), it is easy to show that Z_l can be expressed in terms of our rescaled two-point vertex as follows:

$$Z_l = 1 - \partial_{\mathrm{i}\epsilon}\tilde{\Gamma}_l^{(2)}(Q)|_{Q=0}, \tag{2.33}$$

where $Q = 0$ means $Q = (\alpha, 0, \mathrm{i}0)$. The dimensionless Fermi velocity renormalization factor can be written as

$$\tilde{v}_l = Z_l - \partial_q \tilde{\Gamma}_l^{(2)}(Q)|_{Q=0}. \tag{2.34}$$

Note that for a Fermi liquid $\tilde{v}_l$ can be identified with the dimensionless inverse effective mass renormalization,

$$\tilde{v}_l = \frac{m}{m_l^*}, \tag{2.35}$$

where m is the bare mass and m_l^* is the effective mass of the model with infrared cut-off $\Lambda_0 \mathrm{e}^{-l}$. The expansion of the scaling function associated with the two-point vertex for small q and ϵ then reads

$$\tilde{\Gamma}_l^{(2)}(Q) = \tilde{\mu}_l + (1 - Z_l)\mathrm{i}\epsilon + (Z_l - \tilde{v}_l)q + \mathcal{O}(q^2, \epsilon^2, q\epsilon), \tag{2.36}$$

so that for small q and ϵ the dimensionless inverse propagator defined in equation (2.16) is given by

$$r_l(Q) = Z_l[\mathrm{i}\epsilon - q] + \tilde{\Gamma}_l^{(2)}(Q) = \mathrm{i}\epsilon - \tilde{v}_l q + \tilde{\mu}_l + \mathcal{O}(q^2, \epsilon^2, q\epsilon). \tag{2.37}$$

The exact flow equations for the marginal couplings Z_l and $\tilde{v}_l$ are easily obtained from equations (2.19), (2.21) and (2.34),

$$\partial_l Z_l = -\eta_l Z_l, \tag{2.38}$$

$$\partial_l \tilde{v}_l = -\eta_l \tilde{v}_l - \partial_q \dot{\Gamma}_l^{(2)}(Q)\big|_{Q=0}. \tag{2.39}$$

Differentiating equation (2.19) with respect to $\mathrm{i}\epsilon$, setting $\epsilon = 0$ and using equation (2.33), we see that the flowing anomalous dimension η_l is related to the function $\dot{\Gamma}_l^{(2)}(Q)$ via

$$\eta_l = \partial_{\mathrm{i}\epsilon}\dot{\Gamma}_l^{(2)}(Q)|_{Q=0}. \tag{2.40}$$

Since $\dot{\Gamma}_l^{(2)}$ is defined in terms of the four-point vertex $\tilde{\Gamma}_l^{(4)}$ via equation (2.20), we can obtain the following explicit expression for the flowing anomalous dimension:

$$\eta_l = -\int_{Q'} \dot{G}_l(Q')\partial_{\mathrm{i}\epsilon}\tilde{\Gamma}_l^{(4)}(Q, Q'; Q', Q)|_{Q=0}. \tag{2.41}$$

This expression is also valid in dimensions $d > 1$ provided the discrete index α within $Q = (\alpha, q, \mathrm{i}\epsilon)$ is replaced by a d-dimensional unit vector which labels the points on the

Fermi surface. Thus, for a given irreducible four-point vertex, equation (2.41) can be used to directly calculate the anomalous dimension of any normal Fermi system.

There is one more marginal coupling, namely the irreducible four-point vertex at vanishing momenta and frequencies. Because by construction $\tilde{\Gamma}_l^{(4)}(Q_1', Q_2'; Q_2, Q_1)$ is antisymmetric with respect to the permutation of the incoming or the outgoing fermions, for vanishing external momenta and frequencies the four-point vertex must be of the form

$$\tilde{\Gamma}_l^{(4)}(\alpha_1', 0, \alpha_2', 0; \alpha_2, 0, \alpha_1, 0) = A_{\alpha_1'\alpha_2';\alpha_2\alpha_1}\tilde{g}_l, \tag{2.42}$$

where $A_{\alpha_1'\alpha_2';\alpha_2\alpha_1}$ is defined in equation (2.7). Hence, the marginal part of the four-point vertex can be expressed in terms of a single marginal coupling $\tilde{g}_l$, which satisfies the exact flow equation

$$\partial_l \tilde{g}_l = -2\eta_l \tilde{g}_l + B_l. \tag{2.43}$$

Here B_l is defined by

$$\dot{\Gamma}_l^{(4)}(\alpha_1', 0, \alpha_2', 0; \alpha_2, 0, \alpha_1, 0) = A_{\alpha_1'\alpha_2';\alpha_2\alpha_1}B_l, \tag{2.44}$$

with $\dot{\Gamma}_l^{(4)}$ given in equation (2.28).

3. Approximate solution of the functional flow equations for the two-point vertex

So far no approximation has been made, except for the linearization of the energy dispersion. In order to make progress, we need to truncate the hierarchy of flow equations. We now give a truncation scheme which at weak coupling reproduces the known scaling properties of the spectral function $A(\pm(k_F + p), \omega)$ of the TLM. Moreover, at least for $p = 0$, we recover the exact weak-coupling result for the spectral function known from bosonization.

3.1. One-loop flow

To begin with, let us briefly discuss the flow of the relevant and the marginal couplings within the one-loop approximation. We first consider the two-point vertex. The exact flow equation is given in equation (2.19). The flow is coupled to the irreducible four-point vertex via the inhomogeneity $\dot{\Gamma}_l^{(2)}(Q)$ on the right-hand side, as given in equation (2.20). Within the one-loop approximation, it is sufficient to approximate the four-point vertex appearing in equation (2.20) by

$$\tilde{\Gamma}_l^{(4)}(Q, Q'; Q', Q) = \delta_{\alpha,-\alpha'}\tilde{g}_l + \mathcal{O}(\tilde{g}_l^2), \tag{3.1}$$

where we have used the fact that $A_{\alpha\alpha';\alpha'\alpha} = 1 - \delta_{\alpha,\alpha'} = \delta_{\alpha,-\alpha'}$. In this approximation

$$\dot{\Gamma}_l^{(2)}(Q) = -\tilde{g}_l \int_{Q'} \delta_{\alpha,-\alpha'}\dot{G}_l(Q') + \mathcal{O}(\tilde{g}_l^2) = -\frac{\tilde{g}_l}{2}[\Theta(\tilde{\mu}_l + \tilde{v}_l) + \Theta(\tilde{\mu}_l - \tilde{v}_l)] + \mathcal{O}(\tilde{g}_l^2). \tag{3.2}$$

For $|\tilde{\mu}_l| < |\tilde{v}_l|$ this simplifies to

$$\dot{\Gamma}_l^{(2)}(Q) = -\frac{\tilde{g}_l}{2} + \mathcal{O}(\tilde{g}_l^2), \qquad |\tilde{\mu}_l| < |\tilde{v}_l|. \tag{3.3}$$

As shown below, in the physically relevant case $\tilde{\mu}_l = \mathcal{O}(\tilde{g}_l)$, while $\tilde{v}_l$ is of the order of unity. From equations (2.31) and (2.38)–(2.40) we conclude that up to terms of order $\tilde{g}_l$

$$\partial_l \tilde{\mu}_l = \tilde{\mu}_l - \frac{\tilde{g}_l}{2}, \tag{3.4}$$

$$\partial_l Z_l = 0, \tag{3.5}$$

$$\partial_l \tilde{v}_l = 0. \tag{3.6}$$

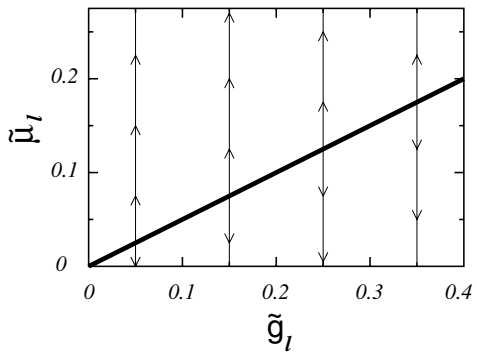

Figure 1. One-loop RG flow in the $\tilde{g}$–$\tilde{\mu}$-plane (see equations (3.4) and (3.7)). The thick solid line is a line of fixed points.

In appendix B we show that the coefficient of order $\tilde{g}_l^2$ in the weak-coupling expansion of the function B_l defined in equation (2.44) vanishes. Since equation (3.5) implies $\eta_l = 0$ at one loop, we obtain from equation (2.43)

$$\partial_l \tilde{g}_l = 0. \tag{3.7}$$

The vanishing of the β-function of the marginal coupling $\tilde{g}_l$ of the TLM is well known [1]. However, the one-loop RG flow of the relevant coupling $\tilde{\mu}_l$ is non-trivial, because the initial value of $\tilde{\mu}_l$ has to be fine-tuned such that $\tilde{\mu}_l$ does not exhibit a runaway flow. As emphasized in [27], the requirement that $\tilde{\mu}_l$ flows into a fixed point is equivalent with the statement that the initial k_F is the correct Fermi momentum, in agreement with the Luttinger theorem [28, 30]. The flow in the $\tilde{g}$–$\tilde{\mu}$-plane implied by equations (3.4) and (3.7) is shown in figure 1. Obviously, at the one-loop level the marginal couplings $\tilde{g}_l$, Z_l and $\tilde{v}_l$ do not flow, while the relevant coupling $\tilde{\mu}_l$ exhibits a runaway flow unless the initial value is chosen such that

$$\tilde{\mu}_0 = \frac{\tilde{g}_0}{2}. \tag{3.8}$$

In this case $\tilde{\mu}_l = \frac{\tilde{g}_0}{2}$ for all l, so that we obtain a RG fixed point. The one-loop flow equations given above have also been discussed by Shankar [4], who derived these equations within the framework of the conventional momentum shell technique. Because within the one-loop approximation $Z_l = 1$, this approximation is not sufficient to detect the non-Fermi-liquid behaviour of our model.

3.2. Two-loop flow of the two-point vertex

It is now straightforward to calculate the full two-point vertex within the two-loop approximation and to study the emergence of Luttinger liquid behaviour when the infrared cut-off is reduced. The crucial point is that for large values of the flow parameter l the momentum- and frequency-dependent part of the four-point vertex can be expanded in powers of the marginal coupling $\tilde{g}_l$. This follows from the fact that the RG trajectory approaches the manifold defined by the relevant and marginal couplings, so that the irrelevant couplings become local functions of the relevant and marginal ones [18, 31].

From equations (2.19) and (2.20) we see that for a two-loop calculation of the irreducible two-point vertex, we need to know the four-point vertex up to order $\tilde{g}_l^2$, i.e. at one-loop level[4].

[4] For the model with the Dirac sea ($\Lambda_0 = \infty$) we explicitly verified [34] $\partial_l \tilde{g}_l = 0$ at two-loop order. We therefore expect a small initial flow of $\tilde{g}_l$ if we keep Λ_0 finite, leading to a fixed-point value $\tilde{g} = \tilde{g}_0 + \mathcal{O}(g_0^3)$. The corrections to the flow of $\tilde{v}_l$ and η_l are beyond two-loop order.

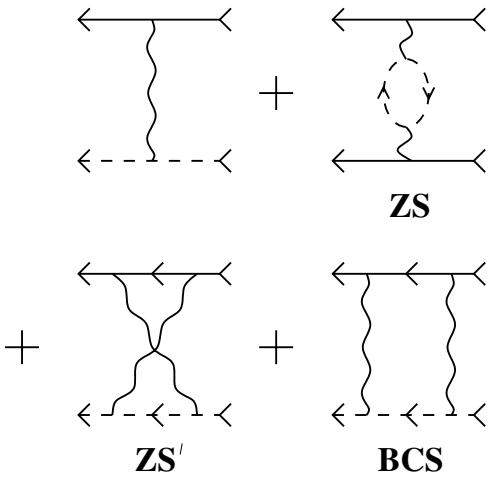

Figure 2. Feynman diagrams contributing to the effective interaction within the one-loop approximation (see equation (3.9)). The solid (dashed) lines represent the fermion propagators with momenta close to the right (left) Fermi point, and the wavy lines represent the flowing coupling constant $\tilde{g}_l$. As the outer legs of the second diagram both correspond to fermions propagating in the same direction, it represents an effective g_4-type interaction.

For $\tilde{\Gamma}_l^{(4)}$ we obtain (see appendix B)

$$\tilde{\Gamma}_l^{(4)}(Q, Q'; Q', Q) = \delta_{\alpha,-\alpha'}\tilde{g}_l + \delta_{\alpha,\alpha'}\tilde{g}_l^2\Pi_l(q-q', \mathrm{i}\epsilon - \mathrm{i}\epsilon') + \delta_{\alpha,-\alpha'}\tilde{g}_l^2[\chi_l(q+q', \mathrm{i}\epsilon - \mathrm{i}\epsilon') + \chi_l(q-q', \mathrm{i}\epsilon + \mathrm{i}\epsilon')], \tag{3.9}$$

with the susceptibilities given by

$$\chi_l(q, \mathrm{i}\epsilon) = -\frac{1}{2\tilde{v}_l}\left\{l\Theta(|q| > \mathrm{e}^l - 1) + \frac{1}{2}\ln\left[\frac{\tilde{v}_l^2(2+|q|)^2 + \epsilon^2}{\tilde{v}_l^2(2-\mathrm{e}^{-l}|q|)^2 + \mathrm{e}^{-2l}\epsilon^2}\right]\Theta(\mathrm{e}^l - 1 > |q|)\right\}, \tag{3.10}$$

and

$$\Pi_l(q, \mathrm{i}\epsilon) = \frac{1}{2}\,\frac{s_q}{\mathrm{i}\epsilon + \tilde{v}_l q}\{(|q|-2)\Theta(\mathrm{e}^l + 1 > |q| > 2) + (2\mathrm{e}^l - |q|)\Theta(2\mathrm{e}^l > |q| > \mathrm{e}^l + 1)\}. \tag{3.11}$$

A graphical representation of equation (3.9) is shown in figure 2. We recognize the usual perturbative contributions to the effective interaction: the first term of order $\tilde{g}_l^2$ on the right-hand side of equation (3.9) corresponds to the contribution from the zero-sound (ZS) channel, the second term corresponds to the Peierls channel (sometimes also denoted by ZS′ channel) and the last term corresponds to the BCS channel. Note that the ZS channel gives rise to an effective retarded forward scattering interaction of the g_4-type (using the g-ology language), which is generated by integrating out degrees of freedom.

To calculate the inhomogeneity $\dot{\Gamma}_l^{(2)}(Q)$ on the right-hand side of the flow equation for the two-point vertex, we now substitute our approximate expression for $\tilde{\Gamma}_l^{(4)}(Q, Q'; Q', Q)$ into equation (2.20). Separating the contributions due to the ZS and the Peierls-BCS (PB) channels, we have

$$\dot{\Gamma}_l^{(2)}(q, \mathrm{i}\epsilon) = -\frac{\tilde{g}_l}{2} + \dot{\Gamma}_l^{(2,\mathrm{ZS})}(q, \mathrm{i}\epsilon) + \dot{\Gamma}_l^{(2,\mathrm{PB})}(q, \mathrm{i}\epsilon) + \mathcal{O}(\tilde{g}_l^3), \tag{3.12}$$

where

$$\dot{\Gamma}_l^{(2,\mathrm{ZS})}(q,\mathrm{i}\epsilon) = -\frac{\tilde{g}_l^2}{2}\int \mathrm{d}q' \int \frac{\mathrm{d}\epsilon'}{2\pi}\frac{\delta(|q'|-1)}{\mathrm{i}\epsilon' - \tilde{v}_l q'}\Pi_l(q-q', \mathrm{i}\epsilon - \mathrm{i}\epsilon')$$
$$= -\frac{\tilde{g}_l^2}{4}s_q\Bigg[\Theta(\mathrm{e}^l > |q| > 1)\frac{|q|-1}{\tilde{v}_l(2+|q|)+\mathrm{i}\epsilon s_q}$$
$$+ \Theta(2\mathrm{e}^l - 1 > |q| > \mathrm{e}^l)\frac{2\mathrm{e}^l - 1 - |q|}{\tilde{v}_l(2+|q|)+\mathrm{i}\epsilon s_q}\Bigg], \tag{3.13}$$

$$\dot{\Gamma}_l^{(2,\mathrm{PB})}(q,\mathrm{i}\epsilon) = -\frac{\tilde{g}_l^2}{2}\int \mathrm{d}q' \int \frac{\mathrm{d}\epsilon'}{2\pi}\frac{\delta(|q'|-1)}{\mathrm{i}\epsilon' - \tilde{v}_l q'}[\chi_l(q+q', \mathrm{i}\epsilon - \mathrm{i}\epsilon') - \chi_l(q-q', \mathrm{i}\epsilon + \mathrm{i}\epsilon')]$$
$$= \frac{\tilde{g}_l^2}{4\tilde{v}_l}s_q\Bigg\{\Theta(1 > |q| > 2 - \mathrm{e}^l)\ln\Bigg[\frac{\tilde{v}_l(4-|q|)+\mathrm{i}\epsilon s_q}{\tilde{v}_l(2\mathrm{e}^l+|q|)+\mathrm{i}\epsilon s_q}\Bigg]$$
$$+ \Theta(\mathrm{e}^l > |q| > 1)\ln\Bigg[\frac{\tilde{v}_l(2+|q|)+\mathrm{i}\epsilon s_q}{\tilde{v}_l(2\mathrm{e}^l+2-|q|)+\mathrm{i}\epsilon s_q}\Bigg]$$
$$- \Theta(\mathrm{e}^l - 2 > |q|)\ln\Bigg[\frac{\tilde{v}_l(4+|q|)-\mathrm{i}\epsilon s_q}{\tilde{v}_l(2\mathrm{e}^l-|q|)-\mathrm{i}\epsilon s_q}\Bigg]\Bigg\}. \tag{3.14}$$

Here, we have introduced the short-hand notation

$$s_q = \mathrm{sign}(q). \tag{3.15}$$

Expanding to first order in q and ϵ, we obtain

$$\dot{\Gamma}_l^{(2,\mathrm{PB})}(q,\mathrm{i}\epsilon) = \frac{\tilde{g}_l^2}{8\tilde{v}_l^2}\Theta(\mathrm{e}^l - 2)[(1-2\mathrm{e}^{-l})\mathrm{i}\epsilon - (1+2\mathrm{e}^{-l})\tilde{v}_l q + \mathcal{O}(\epsilon^2, q^2, \epsilon q)]. \tag{3.16}$$

Because $\dot{\Gamma}_l^{(2,\mathrm{ZS})}(q,\mathrm{i}\epsilon)$ vanishes for $|q| < 1$, it does not contribute to the flow of the marginal couplings Z_l and $\tilde{v}_l$. From equation (2.40) we obtain for the anomalous dimension at scale l

$$\eta_l = \frac{\tilde{g}_l^2}{8\tilde{v}_l^2}\Theta(\mathrm{e}^l - 2)(1-2\mathrm{e}^{-l}), \tag{3.17}$$

and from equation (2.39) we find for the flow of the Fermi velocity renormalization factor

$$\partial_l \tilde{v}_l = \frac{\tilde{g}_l^2}{2\tilde{v}_l}\Theta(\mathrm{e}^l - 2)\mathrm{e}^{-l}. \tag{3.18}$$

Using the fact that $\tilde{g}_l = \tilde{g}$ is independent of the flow parameter l, equation (3.18) can be easily integrated,

$$\tilde{v}_l = \tilde{v}_0\Bigg[1 + \Theta(\mathrm{e}^l - 2)\frac{\tilde{g}^2}{2\tilde{v}_0^2}(1-2\mathrm{e}^{-l})\Bigg]^{1/2}. \tag{3.19}$$

Note that $\tilde{v}_l$ rapidly approaches a constant $\tilde{v}_\infty$ for large l, which is to leading order in $\tilde{g}$ given by

$$\tilde{v}_\infty = \tilde{v}_0 + \frac{\tilde{g}^2}{4\tilde{v}_0} + \mathcal{O}(\tilde{g}_0^4). \tag{3.20}$$

In figure 3 we show the flow of the anomalous dimension η_l given in equation (3.17) as a function of the logarithmic flow parameter l. Obviously, η_l vanishes for $l < \ln 2$, and approaches a constant η for large l, which is given by

$$\eta = \frac{\tilde{g}^2}{8\tilde{v}_\infty}. \tag{3.21}$$

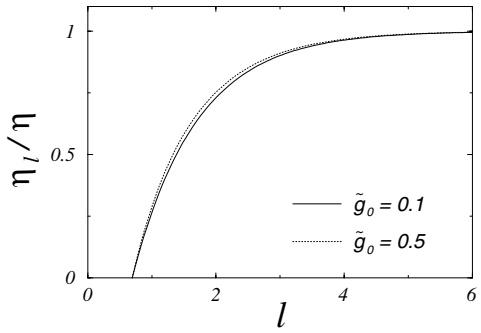

Figure 3. Anomalous dimension η_l as a function of the logarithmic flow parameter l (see equations (3.17) and (3.18)).

In [32] this result has been derived within the field theory RG. The above fixed point value of η agrees with the weak-coupling expansion of the bosonization result for the anomalous dimension of the spinless g_2-TLM. Note, however, that the exact solubility of the TLM relies on the filled Dirac sea associated with the linearized energy dispersion. As discussed by Schulz and Shastry [29], the introduction of the Dirac sea leads to finite renormalizations of the fixed point values of the Luttinger liquid parameters (such as the anomalous dimension), so that the value of η beyond the leading order $\tilde{g}^2$ is modified. This can be explicitly verified within our RG approach, where the introduction of the Dirac sea corresponds to the removal of the ultraviolet cut-off Λ_0. Then we should take the limit $e^l \to \infty$ in equations (3.13) and (3.14), so that the explicit l-dependence on the right-hand sides of these expressions disappears. In this case the marginal coupling $\tilde{v}_l$ is not renormalized at all ($\partial_l \tilde{v}_l = 0$), so that $\tilde{v}_\infty = \tilde{v}_0$. Furthermore, the initial flow of the anomalous dimension η_l discussed above is also removed by the Dirac sea, so that η_l is effectively replaced by its asymptotic limit η given in equation (3.21). To simplify the following calculation of the spectral function, we shall from now on work with a Dirac sea, which formally amounts to taking the limit $l \to \infty$ in equations (3.13) and (3.14). The result is displayed in appendix C, equations (C.1) and (C.2).

So far we have calculated the function $\dot{\Gamma}_l^{(2)}(Q)$ perturbatively to second order in $\tilde{g}_0$. Let us for the moment proceed further within perturbation theory. In this case we may set $\eta_l = 0$ on the right-hand side of the exact flow equation (2.19) for the two-point vertex, which amounts to setting $\bar{\eta}_l(t) = 0$ in equation (2.25). As explained in [31], in our formalism it is necessary to introduce *subtracted* vertices $\tilde{\Gamma}_l^{(2n,sub)}$ which solely contain the irrelevant parts of the vertex function (for explicit definitions see appendix A). The flow equations for the subtracted vertices are formally identical with the flow equations for the un-subtracted vertices, except for the fact that the inhomogeneities $\dot{\Gamma}_l^{(2n)}$ have to be replaced by their subtracted versions $\dot{\Gamma}_l^{(2n,sub)}$. Introducing the Dirac sea and assuming that initially $\tilde{\Gamma}_{l=0}^{(2,sub)}(Q) = 0$ we may approximate

$$\tilde{\Gamma}_l^{(2,sub)}(q, \mathrm{i}\epsilon) \approx \int_0^l \mathrm{d}t\, \mathrm{e}^t \dot{\Gamma}_\infty^{(2,sub)}(\mathrm{e}^{-t}q, \mathrm{e}^{-t}\mathrm{i}\epsilon) = \int_{\mathrm{e}^{-l}}^1 \mathrm{d}\lambda\, \lambda^{-2} \dot{\Gamma}_\infty^{(2,sub)}(\lambda q, \lambda \mathrm{i}\epsilon). \tag{3.22}$$

Substituting the perturbative result for $\dot{\Gamma}_\infty^{(2,sub)}(q, \mathrm{i}\epsilon)$ given in equation (C.3) into (3.22), going back to the physical variables $p = \Lambda q / v_F$, $\omega = \Lambda \epsilon$, using equation (2.17) and finally taking the scaling limit $l \to \infty$ (i.e. $\Lambda \to 0$), we recover the perturbative self-energy of the spinless g_2-TLM [11],

$$\Sigma(\alpha k_F + \alpha p, \mathrm{i}\omega) - \Sigma(\alpha k_F, \mathrm{i}\omega) \approx -\frac{\tilde{g}^2}{8} v_F p + \frac{\tilde{g}^2}{16}(\mathrm{i}\omega - v_F p) \ln\left[\frac{(v_F p)^2 + \omega^2}{\xi_0^2}\right]. \tag{3.23}$$

Let us now consider the *scaling regime*. Note that $\tilde{\Gamma}_l^{(2,sub)}$ in equation (3.22) still depends explicitly on the logarithmic scale factor l. However, it is easy to check that in the regime

$$1 \ll |q| \ll \mathrm{e}^l, \qquad 1 \ll |\epsilon| \ll \mathrm{e}^l, \tag{3.24}$$

we may approximate

$$\tilde{\Gamma}_l^{(2,sub)}(q, \mathrm{i}\epsilon) \approx \tilde{\Gamma}_{l\to\infty}^{(2,sub)}(q, \mathrm{i}\epsilon), \tag{3.25}$$

so that the only l-dependence of the self-energy enters via $q = p\xi = p\xi_0 \mathrm{e}^l$ and $\epsilon = \omega\tau = \omega/\Lambda = \omega \mathrm{e}^l/\Lambda_0$. Thus, in the scaling region (3.24) the spectral function can be written in terms of a function that depends on l only implicitly via the scaling variables: this is in agreement with the dynamic scaling hypothesis [13] applied to the single-particle Green function of our model.

We now propose a simple procedure to go beyond perturbation theory: from equation (2.25) we know that the exact two-point vertex for $l \gg 1$ satisfies

$$\tilde{\Gamma}_l^{(2,sub)}(q, \mathrm{i}\epsilon) = \int_0^l \mathrm{d}t\, \mathrm{e}^{(1-\eta)t} \dot{\Gamma}_\infty^{(2,sub)}(\mathrm{e}^{-t}q, \mathrm{e}^{-t}\mathrm{i}\epsilon) = \int_{e^{-l}}^1 \mathrm{d}\lambda\, \lambda^{-2+\eta} \dot{\Gamma}_\infty^{(2,sub)}(\lambda q, \lambda \mathrm{i}\epsilon), \tag{3.26}$$

which differs from the perturbative expression (3.22) because the fixed-point value of the anomalous dimension appears on the right-hand side. In appendix C we show that the flow function $\dot{\Gamma}_\infty^{(2,sub)}(q, \mathrm{i}\epsilon)$ on the right-hand side of equation (3.26) may be approximated by

$$\begin{aligned}\dot{\Gamma}_\infty^{(2,sub)}(q, \mathrm{i}\epsilon) \approx \eta s_q \Big\{ & 2\Theta(|q| > 1) \ln[\tilde{v}(2 + |q|) + \mathrm{i}\epsilon s_q] + 2\Theta(1 > |q|) \ln[\tilde{v}(4 - |q|) + \mathrm{i}\epsilon s_q] \\ & - 2\ln[\tilde{v}(4 + |q|) - \mathrm{i}\epsilon s_q] - \Theta(|q| > 1) \frac{3\tilde{v}|q| + \mathrm{i}\epsilon s_q}{\tilde{v}(2 + |q|) + \mathrm{i}\epsilon s_q} - (\mathrm{i}\epsilon s_q - \tilde{v}|q|) \Big\}.\end{aligned} \tag{3.27}$$

This expression is almost identical with the perturbative two-loop result (C.3), except that the term $\eta s_q \Theta(|q| > 1)$ has been omitted, and the factor $\tilde{v}_0$ has been replaced by the perturbative Fermi velocity renormalization factor

$$\tilde{v} = 1 - \frac{\tilde{g}^2}{8} = 1 - \eta \tag{3.28}$$

(see equation (1.4)). Note that within perturbation theory the term $\eta s_q \Theta(|q| > 1)$ in equation (C.3) is responsible for the finite Fermi velocity renormalization given by the first term $-\frac{\tilde{g}^2}{8} v_F p$ on the right-hand side of equation (3.23). By substituting $\tilde{v}_0 \to \tilde{v}$ in equation (C.3), we have implicitly replaced the bare propagator in the scaling limit by $[\mathrm{i}\epsilon - \tilde{v}q]^{-1}$, thus taking the Fermi velocity renormalization in the scaling limit self-consistently into account.

Given equations (3.26) and (3.27), we may calculate the complete dynamic scaling function for the irreducible self-energy, describing the change in scaling behaviour as we move from the hydrodynamic into the scaling regime. In the hydrodynamic regime the scaling function is analytic in q and ϵ. On the other hand, for large $|q|$ and $|\epsilon|$ the scaling function exhibits algebraic singularities corresponding to Luttinger liquid behaviour. In the scaling regime (3.24) we may use the approximation (3.25) and obtain from equations (3.26) and (3.27)

$$\begin{aligned}\tilde{\Gamma}_\infty^{(2,sub)}(q, \mathrm{i}\epsilon) = \frac{\eta}{2}(\mathrm{i}\epsilon - \tilde{v}q) \Bigg\{ & F\left(\frac{\mathrm{i}\epsilon s_q - \tilde{v}|q|}{4\tilde{v}}\right) + F\left(-\frac{\mathrm{i}\epsilon s_q + \tilde{v}|q|}{2\tilde{v}}\right) \\ & + |q|^{-\eta}\left[F\left(-\frac{\mathrm{i}\epsilon s_q - \tilde{v}|q|}{4\tilde{v}|q|}\right) - F\left(-\frac{\mathrm{i}\epsilon s_q + \tilde{v}|q|}{2\tilde{v}|q|}\right)\right]\Bigg\},\end{aligned} \tag{3.29}$$

where the complex function $F(z)$ is defined by

$$F(z) = z \int_0^1 \mathrm{d}\lambda \frac{\lambda^\eta}{1 - z\lambda} = z\, {}_2F_1(1, 1 + \eta, 2 + \eta; z). \tag{3.30}$$

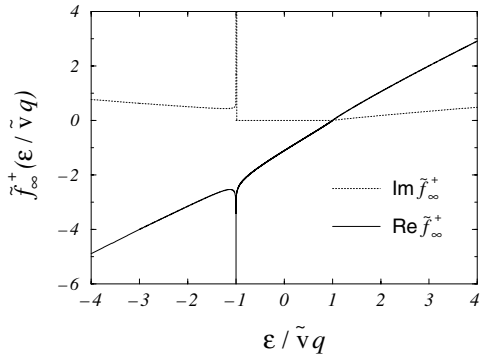

Figure 4. Real and imaginary parts of $\tilde{f}^{+}_{\infty}(\epsilon/\tilde{v}q) \equiv r_{\infty}(q, \epsilon + \mathrm{i}0)/|q|^{1-\eta} = [(\epsilon - \tilde{v}q) + \tilde{\Gamma}^{(2,sub)}_{\infty}(q, \epsilon + \mathrm{i}0)]/|q|^{1-\eta}$ for $\eta = 0.2$, where $\tilde{\Gamma}^{(2,sub)}_{\infty}(q, \epsilon + \mathrm{i}0)$ is the subtracted irreducible two-point scaling function (see equations (C.5) and (C.7)).

Here, ${}_2F_1(a, b, c; z)$ is the Gauss hypergeometric function. Note that equation (3.29) is restricted to the scaling regime defined by (3.24). To obtain the spectral function, we analytically continue $\tilde{\Gamma}^{(2,sub)}_{\infty}(q, \mathrm{i}\epsilon)$ according to $\mathrm{i}\epsilon \to \epsilon + \mathrm{i}0$. The result is given in appendix C, equations (C.5) and (C.7).

From equation (C.7) we see that the leading contribution of the real part exactly cancels the inverse bare propagator $\mathrm{i}\epsilon - \tilde{v}q$ such that $r_{\infty}(q, \epsilon + \mathrm{i}0) = (\epsilon - \tilde{v}q) + \tilde{\Gamma}^{(2,sub)}_{\infty}(q, \epsilon + \mathrm{i}0)$ for $q \neq 0$ has the dynamic scaling property [13]

$$r_{\infty}(q, \epsilon + \mathrm{i}0) = |q|^{1-\eta} \tilde{f}^{\pm}_{\infty}(\epsilon/\tilde{v}q), \tag{3.31}$$

with

$$\mathrm{Re}\, \tilde{f}^{\pm}_{\infty}(x) = \pm(x-1)\left\{\Theta(x > 3)\frac{1}{2}\left[\left|\frac{x-1}{4}\right|^{-\eta} + \left|\frac{x+1}{2}\right|^{-\eta}\right] + \Theta(-3 > x)\left|\frac{x-1}{4}\right|^{-\eta}\right\}, \tag{3.32}$$

and

$$\mathrm{Im}\, \tilde{f}^{\pm}_{\infty}(x) = 2\pi\eta\left\{\Theta(x > 1)\left|\frac{x-1}{4}\right|^{1-\eta} + \Theta(-1 > x > -3)\left|\frac{x-1}{4}\right|\left|\frac{x+1}{2}\right|^{-\eta} + \Theta(-3 > x)\left|\frac{x-1}{4}\right|^{1-\eta}\right\}. \tag{3.33}$$

Here, the functions $\tilde{f}^{+}_{\infty}(x)$ and $\tilde{f}^{-}_{\infty}(x)$ refer to $q > 0$ and $q < 0$ respectively and a graph of $\tilde{f}^{+}_{\infty}(\epsilon/\tilde{v}q)$ is shown for $\eta = 0.2$ in figure 4. Using the fact that for $\xi \gg \xi_0$ we may identify

$$Z_l = Z_0 \mathrm{e}^{-\int_0^l \mathrm{d}t\, \eta_t} \equiv \bar{Z}_0 \mathrm{e}^{-\eta l} \approx \left(\frac{\xi_0}{\xi}\right)^{\eta}, \tag{3.34}$$

where the constant $\bar{Z}_0 = \mathcal{O}(1)$ has been absorbed by ξ_0, the corresponding spectral function can be written in the scaling form similar to equation (1.9),

$$A(\alpha(k_F + p), \omega) = \tau\left(\frac{\xi_0}{\xi}\right)^{\eta} \tilde{A}_{\infty}(p\xi, \omega\tau), \tag{3.35}$$

where $\tau = \xi/v_F = 1/\Lambda$, and the scaling function $\tilde{A}_{\infty}(q, \epsilon)$ is given by

$$\tilde{A}_{\infty}(q, \epsilon) = -\frac{1}{\pi}\mathrm{Im}[\epsilon - \tilde{v}q + \tilde{\mu}_{\infty} + \tilde{\Gamma}^{(2,sub)}_{\infty}(q, \epsilon + \mathrm{i}0)]^{-1}. \tag{3.36}$$

Using equation (3.31), for $q \neq 0$ this can again be written in scaling form

$$\tilde{A}_\infty(q,\epsilon) = |q|^{\eta-1}\tilde{h}_\infty(\epsilon/\tilde{v}q), \tag{3.37}$$

with

$$\tilde{h}_\infty(x) = \frac{\eta}{2}|x-1|^{\eta-1}\begin{cases} 4\left[1+\left|\dfrac{x-1}{x+1}\right|^{\eta}\right]^{-2} & \text{for } x > 1 \\ 0 & \text{for } 1 > x > -1 \\ 4\left[\left|2\dfrac{x+1}{x-1}\right|^{\eta/2} + \left|\dfrac{1}{2}\dfrac{x-1}{x+1}\right|^{\eta/2}\right]^{-2} & \text{for } -1 > x > -3 \\ 1 & \text{for } -3 > x. \end{cases} \tag{3.38}$$

In the prefactor we have retained only the leading order in η. For $q = 0$, the dynamic scaling function reduces to

$$\tilde{A}_\infty(0,\epsilon) = \frac{\eta}{2}|\epsilon|^{\eta-1}. \tag{3.39}$$

A plot of the dynamic scaling function $\tilde{h}_\infty(\epsilon/\tilde{v}q)$ is given in figure 5 for $\eta = 0.2$. For a comparison, we have also plotted the generally accepted scaling function of the TLM, given in equation (1.7). The qualitative agreement between the two plots becomes even better for smaller η: we chose $\eta = 0.2$ to amplify the differences[5]. Recall that equation (3.38) has been derived for $|q| \gg 1$, $|\epsilon| \gg 1$ *and for large* $||\epsilon| - \tilde{v}|q||$. In this limit the small constant $\tilde{\mu}_\infty$ on the right-hand side of equation (3.38) can be neglected. In terms of the physical variables $p = q/\xi$ and $\omega = \epsilon/\tau = \epsilon v_F/\xi$ the condition $||\epsilon| - \tilde{v}|q|| \gg 1$ becomes $||\omega| - v_c|p|| \gg 1/\tau$, where $v_c = \tilde{v}v_F$. Using the fact that the function $\tilde{A}_\infty(q,\epsilon)$ is a homogeneous function of degree $\eta - 1$, i.e.

$$\tilde{A}_\infty(sq, s\epsilon) = s^{\eta-1}\tilde{A}_\infty(q,\epsilon), \tag{3.40}$$

we may write $\tilde{A}_\infty(p\xi, \omega\tau) = \tau^{\eta-1}\tilde{A}_\infty(v_F p, \omega)$. With $\tau(\xi_0/\xi)^\eta\tau^{\eta-1} = \Lambda_0^{-\eta}$ we finally obtain for the spectral function at the Luttinger liquid fixed point,

$$A(\alpha(k_F + p), \omega) = \Lambda_0^{-\eta}|v_c p|^{\eta-1}\tilde{h}_\infty(\omega/v_c p) \qquad \text{for } p \neq 0 \tag{3.41}$$

and

$$A(\alpha k_F, \omega) = \Lambda_0^{-\eta}\frac{\eta}{2}|\omega|^{\eta-1}, \qquad \text{for } p = 0. \tag{3.42}$$

Let us now compare our results with those obtained via bosonization for the TLM. First of all, setting $p = 0$ in equation (1.2) we obtain exact agreement with equation (3.42). Thus, at least for $p = 0$, our truncation of the exact RG flow equations is reliable. Moreover, equation (3.41) exhibits the same scaling behaviour $A(\alpha k_F + \alpha sp, s\omega) = s^{\eta-1}A(\alpha k_F + \alpha p, \omega)$ as the expression (1.2) obtained via bosonization. For finite p, however, the detailed lineshape of the spectral function predicted by equation (3.41) is different from equation (1.2). In particular, for $\omega \to v_c p + 0$ the bosonization result (1.2) predicts

$$A_{TL}(k_F + p, \omega) \sim \Lambda_0^{-\eta}\frac{\eta}{2}|2v_c p|^{\eta/2}|\omega - v_c p|^{-1+\eta/2}, \tag{3.43}$$

while our RG calculation yields

$$A(k_F + p, \omega) \sim \Lambda_0^{-\eta}2\eta|\omega - v_c p|^{-1+\eta}, \tag{3.44}$$

[5] Note that because $\eta \approx \tilde{g}^2/8$ the value $\eta = 0.2$ corresponds to $\tilde{g} \approx 1.3$ which is out of range of a weak-coupling expansion. Choosing $\tilde{g} = 0.3$ leads to $\eta \approx 0.01$ in which case the two plots are indeed indistinguishable.

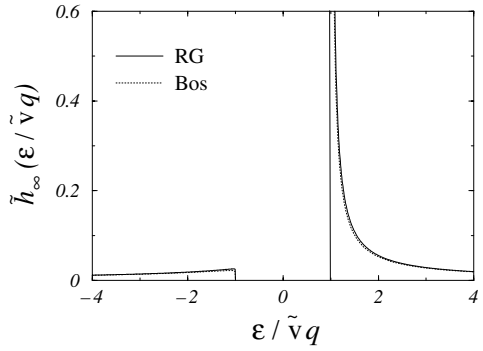

Figure 5. Graph of the dynamic scaling function $\tilde{h}_\infty(\epsilon/\tilde{v}q) \equiv \tilde{A}_\infty(q,\epsilon)/|q|^{\eta-1}$ for $\eta = 0.2$ (see equations (3.35) and (3.38)). For smaller η the RG result is indistinguishable from the bosonization result $\tilde{h}_{TL}(\epsilon/\tilde{v}q)$ on this scale.

which diverges with a different exponent than equation (3.43). Similarly, for $\omega \to -v_c p - 0$ the bosonization result (1.2) predicts

$$A_{TL}(k_F + p, \omega) \sim \Lambda_0^{-\eta} \frac{\eta}{2} |2v_c p|^{-1+\eta/2} |\omega + v_c p|^{\eta/2}, \tag{3.45}$$

while equation (3.41) yields

$$A(k_F + p, \omega) \sim \Lambda_0^{-\eta} 2\eta |2v_c p|^{-1} |\omega + v_c p|^{\eta}. \tag{3.46}$$

Hence the degree of divergence of the singularities at $\omega = \pm v_c p$ is slightly different from the bosonization result. The reason for these deviations remains unclear to us. It might be due to the replacement of the full interacting propagators appearing in the loop-integrations of the inhomogeneities $\dot{\Gamma}_l^{(2)}$ and $\dot{\Gamma}_l^{(4)}$, by the bare propagator, see equation (B.2). To improve our result $\tilde{\Gamma}_l^{(2)}$ should be calculated self-consistently, which we have not been able to do analytically.

Note that equation (3.44) has been derived assuming $|\epsilon^2 - \tilde{v}^2 q^2| \gg 1$, which means in terms of the physical variables $||\omega| - v_c|p|| \gg 1/\tau = \Lambda$. For $\Lambda \to 0$ this condition is always satisfied unless precisely $\omega = \pm v_c p$. This limiting procedure describes the spectral function precisely at the critical point, because the length $\xi = v_F/\Lambda$ associated with the infrared cut-off can be sent to infinity before the limit $\omega \to v_c p$ is taken.

In fact there exists another regime (corresponding to a different physical situation) where both $|\epsilon| = |\omega|\tau$ and $|q| = |p|\xi$ are large, but where

$$\big||\epsilon| - \tilde{v}|q|\big| \lesssim 1. \tag{3.47}$$

In this case we first take the limit $\omega \to \pm v_c p$, and then remove the infrared cut-off $\Lambda = 1/\tau \to 0$, leading to a spectral function that behaves completely differently. Keeping in mind that in practice the TLM describes a physical system only above some finite energy scale Λ_* below which backscattering becomes important or a crossover to higher dimensionality sets in, this limiting procedure is physically relevant to describe quasi-one-dimensional systems. If we naively use our result for the irreducible self-energy given in equation (3.29), we find with the help of equation (C.6) that for $\epsilon \to \tilde{v}q$ and for small η

$$\tilde{\Gamma}_\infty^{(2,sub)}(q, \mathrm{i}\epsilon) \approx \frac{|q|^{-\eta}}{2} (\mathrm{i}\epsilon - \tilde{v}q). \tag{3.48}$$

Since by assumption $|q| \gg 1$, this is a negligible correction to the bare inverse propagator $\mathrm{i}\epsilon - \tilde{v}q$. It follows that in this regime our scaling function is simply

$$\tilde{A}_\infty(q, \epsilon) \approx \delta(\epsilon - \tilde{v}q + \tilde{\mu}_\infty). \tag{3.49}$$

Using equation (3.35) this may be written in the form

$$A(k_F + p, \omega) \approx Z_{l_*} \delta(\omega - v_c p), \tag{3.50}$$

so that the spectral function exhibits a small but still finite quasiparticle peak with a weight of the order of $Z_{l_*} = (\Lambda_*/\Lambda_0)^\eta$. This quasiparticle peak is due to the finite crossover energy scale Λ_* and does not occur in the TLM, where $\Lambda_* = 0$ at zero temperature and where the infrared cut-off Λ can be reduced to zero. Note that our result for Z_{l_*} is in qualitative agreement with that of [33], where a transverse hopping parameter $t_\perp$ (that appears to be a *relevant* perturbation of the Luttinger liquid state) is taken into account. In this case we should identify $\Lambda_* \sim t_\perp$. In deriving equation (3.49) we have introduced the Dirac sea and ignored the non-linearity in the energy dispersion as well as other irrelevant couplings, which will broaden the δ-function. In principle all these effects can be systematically taken into account within our formalism. The calculations are quite tedious and are beyond the scope of this work.

4. Summary and conclusions

In this work we have shown how to calculate the momentum- and frequency-dependent single-particle spectral function by means of a particular version of the functional RG method [27]. For simplicity, we have applied this method to the exactly solvable TLM. Our truncation scheme of the exact hierarchy of RG flow equations consists of the following steps.

(1) Calculate the flow of the relevant and marginal couplings perturbatively for small interactions and adjust the initial values such that the RG flow approaches a fixed point.
(2) Calculate the momentum- and frequency-dependent part of the four-point vertex (which involves an infinite number of irrelevant couplings) in powers of the marginal part of the four-point vertex.
(3) Calculate the anomalous dimension in powers of the marginal part of the four-point vertex.
(4) Substitute the results of steps 2 and 3 into the exact flow equation of the two-point vertex and then solve this equation exactly.

The result for the spectral function $A(k, \omega)$ is quite encouraging: it has the correct scaling properties, and for $k = \pm k_F$ agrees with the exact bosonization result. For finite $k - k_F$ and ω, we have found evidence that the spectral line shape in the vicinity of the Luttinger liquid fixed point exhibits some non-universal features.

Our work also shows how non-Fermi-liquid behaviour in a strongly correlated Fermi system can be detected using modern functional RG methods. In this case the *rescaling* step of the RG transformation is essential and must not be neglected within two-loop calculations. The crucial point is that the renormalized vertices involve wavefunction renormalization factors (see equation (2.18)), which for a strongly correlated system can cancel a possibly strong enhancement of the unrescaled vertices. Our simple one-dimensional model allows us to study such a scenario in detail. In this case $\Gamma^{(4)}_\Lambda$ can be parametrized in terms of a single marginal coupling g_l, which is defined in analogy to equations (2.6) and (2.42),

$$\Gamma^{(4)}_{\Lambda_0 e^{-l}}(\alpha_1' k_F, 0, \alpha_2' k_F, 0; \alpha_2 k_F, 0, \alpha_1 k_F, 0) = A_{\alpha_1'\alpha_2';\alpha_2\alpha_1} g_l. \tag{4.1}$$

At the two-loop order, the flow equation of g_l for our model is [34]

$$\partial_l g_l = \frac{\nu_0^2}{4} g_l^3. \tag{4.2}$$

This implies

$$g_l = \frac{g_0}{\sqrt{1 - \frac{\nu_0^2}{2} g_0^2 l}}. \tag{4.3}$$

Obviously, g_l diverges at a finite scale $l_* = 2/(\nu_0 g_0)^2$. However, this divergence and the associated runaway-flow to strong coupling are unphysical, because the coupling g_l in equation (4.1) is *not* the properly renormalized coupling that can be identified with the usual g_2-interaction of the TLM. The latter is defined as a model describing the *fixed point* of the RG. Thus, the g_2-coupling that appears in the TLM should be identified with the *renormalized coupling at the RG fixed point*, which is related to the fixed point value of our rescaled coupling $\tilde{g}_l$,

$$\nu_0 g_2 = \lim_{l\to\infty} \tilde{g}_l = \lim_{l\to\infty} [Z_l^2 \nu_0 g_l] \tag{4.4}$$

(see equations (2.18) and (2.42)). Similar relations between vertex functions and interaction parameters at the RG fixed point are well known from Landau–Fermi liquid theory [35]. In our simple model with a linearized energy dispersion the two-loop flow equation of the rescaled coupling is simply $\partial_l \tilde{g}_l = 0$, so that the limit $l \to \infty$ in equation (4.4) indeed exists. Note that the vanishing wavefunction renormalization factor Z_l exactly compensates the diverging unrescaled coupling g_l such that the rescaled coupling $\tilde{g}_l$ remains finite and small. We believe that the above interpretation of the runaway flow of the RG-flow equations for the marginal part of the unrescaled vertices $\Gamma_\Lambda^{(4)}$ is not only specific to one dimension, where the RG fixed point does not correspond to a Fermi liquid. Assuming that in two dimensions the RG fixed point corresponds to a strongly correlated Fermi liquid with $Z_\infty \ll 1$, we expect that the unrescaled vertices given in equation (4.1) will flow to a finite but large value, which numerically might be indistinguishable from a runaway flow to infinity. At the same time, the properly rescaled vertices $\tilde{\Gamma}_l^{(4)}$ defined in equation (2.18) can remain finite and small.

The problem of calculating correlation functions of many-body systems at finite wavevectors or frequencies using RG methods has not received much attention. For classical systems, functional RG calculations of the momentum dependence of correlation functions can be found in the textbook by Ivanchenko and Lisyansky [36]. Here we have presented a functional RG calculation of a momentum- and frequency-dependent correlation function of a non-trivial quantum mechanical many-body system. For a special two-dimensional system a similar calculation has recently been performed by Ferraz [16], who used the field theory RG. We believe that the method described in this work will also be useful to study other problems where no exact solutions are available. For example, the spectral function of one-dimensional Fermi systems where backscattering or Umklapp scattering are relevant cannot be calculated exactly by means of bosonization or other methods. Using our RG method, it should be possible to obtain the spectral function of Luther–Emery liquids even away from the Luther–Emery point.

Acknowledgments

We thank A Ferraz, V Meden and K Schönhammer for discussions. This work was partially supported by the DFG via Forschergruppe FOR 412.

Appendix A. Subtracted vertices

In this appendix we give the explicit definitions of the subtracted vertex functions. For the two-point vertex we have to subtract the relevant part related to $\tilde{\mu}_l$ and the marginal parts related to Z_l and $\tilde{v}_l$ (see equations (2.30), (2.33) and (2.34)),

$$\begin{aligned}\tilde{\Gamma}_l^{(2,sub)}(Q) &= \tilde{\Gamma}_l^{(2)}(Q) - \tilde{\Gamma}_l^{(2)}(\alpha, 0, \mathrm{i}0) - \mathrm{i}\epsilon\, \partial_{\mathrm{i}\epsilon} \tilde{\Gamma}_l^{(2)}(Q)\big|_{Q=0} - q\, \partial_q \tilde{\Gamma}_l^{(2)}(Q)\big|_{Q=0} \\ &= \tilde{\Gamma}_l^{(2)}(Q) - \tilde{\mu}_l - \mathrm{i}\epsilon(1 - Z_l) - q(Z_l - \tilde{v}_l). \end{aligned} \tag{A.1}$$

The rescaled inverse propagator $r_l(q, \mathrm{i}\epsilon)$ defined in equation (2.16) can then be written as

$$r_l(q, \mathrm{i}\epsilon) = \mathrm{i}\epsilon - \tilde{v}_l q + \tilde{\mu}_l + \tilde{\Gamma}_l^{(2,sub)}(Q). \tag{A.2}$$

For the irrelevant part of the four-point vertex we have to subtract the marginal coupling $\tilde{g}_l$,

$$\begin{aligned}\tilde{\Gamma}_l^{(4,sub)}(Q_1', Q_2'; Q_2, Q_1) &= \tilde{\Gamma}_l^{(4)}(Q_1', Q_2'; Q_2, Q_1) - \tilde{\Gamma}_l^{(4)}(Q_1', Q_2'; Q_2, Q_1)|_{q_i=\epsilon_i=0} \\ &= \tilde{\Gamma}_l^{(4)}(Q_1', Q_2'; Q_2, Q_1) - A_{\alpha_1'\alpha_2';\alpha_2\alpha_1}\tilde{g}_l. \end{aligned}\tag{A.3}$$

As explained in section 3.2, for the flow of the subtracted vertices we also need to introduce subtracted versions of the corresponding inhomogeneities,

$$\dot{\Gamma}_l^{(2,sub)}(Q) = \dot{\Gamma}_l^{(2)}(Q) - \dot{\Gamma}_l^{(2)}(\alpha, 0, \mathrm{i}0) - \mathrm{i}\epsilon\partial_{\mathrm{i}\epsilon}\dot{\Gamma}_l^{(2)}(Q)|_{Q=0} - q\partial_q\dot{\Gamma}_l^{(2)}(Q)|_{Q=0} \tag{A.4}$$

for the two-point vertex, and

$$\dot{\Gamma}_l^{(4,sub)}(Q_1', Q_2'; Q_2, Q_1) = \dot{\Gamma}_l^{(4)}(Q_1', Q_2'; Q_2, Q_1) - \dot{\Gamma}_l^{(4)}(Q_1', Q_2'; Q_2, Q_1)|_{Q_i=Q_i'=0} \tag{A.5}$$

for the four-point vertex.

Appendix B. One-loop calculation of the four-point vertex

Here we display the relevant parts of the calculation leading to the one-loop result for the four-point vertex, equations (3.9)–(3.11).

For a one-loop calculation of $\tilde{\Gamma}_l^{(4)}$ we need to retain all terms in the flow equation (2.27) up to order $\tilde{g}_l^2$. Using the fact that $\tilde{\Gamma}_l^{(6)}$ is of order $\tilde{g}_l^3$ and hence can be neglected [18, 31], we obtain from equation (2.28) to second order in $\tilde{g}_l$

$$\begin{aligned}&\dot{\Gamma}_l^{(4)}(Q_1', Q_2'; Q_2, Q_1) \\ &\quad\approx -\tilde{g}_l^2\int_Q\Big\{\frac{1}{2}[A_{\alpha_1'\alpha_2';\alpha'\alpha}A_{\alpha\alpha';\alpha_2\alpha_1}(\dot{G}_l(Q)\tilde{G}_l(Q') + \tilde{G}_l(Q)\dot{G}_l(Q'))]_{K'=K_1+K_2-K} \\ &\qquad - [A_{\alpha_1'\alpha';\alpha\alpha_1}A_{\alpha_2'\alpha;\alpha'\alpha_2}(\dot{G}_l(Q)\tilde{G}_l(Q') + \tilde{G}_l(Q)\dot{G}_l(Q'))]_{K'=K+K_1-K_1'} \\ &\qquad + [A_{\alpha_2'\alpha';\alpha\alpha_1}A_{\alpha_1'\alpha;\alpha'\alpha_2}(\dot{G}_l(Q)\tilde{G}_l(Q') + \tilde{G}_l(Q)\dot{G}_l(Q'))]_{K'=K+K_1-K_2'}\Big\}. \end{aligned}\tag{B.1}$$

Because on the critical manifold $\tilde{\mu}_l = \mathcal{O}(\tilde{g}_l)$, we may approximate on the right-hand side of equation (B.1)

$$\tilde{G}_l(Q) \approx \frac{\Theta(\mathrm{e}^l > |q| > 1)}{\mathrm{i}\epsilon - \tilde{v}_l q}, \qquad \dot{G}_l(Q) \approx \frac{\delta(|q| - 1)}{\mathrm{i}\epsilon - \tilde{v}_l q}. \tag{B.2}$$

Note that this amounts to a one-loop calculation, taking $\tilde{v}_l$ self-consistently into account. The integrations in equation (B.1) can then be performed. We obtain

$$\begin{aligned}\dot{\Gamma}_l^{(4)}(Q_1', Q_2'; Q_2, Q_1) \approx -\tilde{g}_l^2\{&A_{\alpha_1'\alpha_2';\alpha_2\alpha_1}\dot{\chi}_l(q_1 - q_2, \mathrm{i}\epsilon_1 + \mathrm{i}\epsilon_2) \\ &+ E_{\alpha_1'\alpha_2';\alpha_2\alpha_1}[\delta_{\alpha_1,\alpha_2}\dot{\Pi}_l(q_1 - q_1', \mathrm{i}\epsilon_1 - \mathrm{i}\epsilon_1') + \delta_{\alpha_1,-\alpha_2}\dot{\chi}_l(q_1 + q_1', \mathrm{i}\epsilon_1 - \mathrm{i}\epsilon_1')] \\ &- D_{\alpha_1'\alpha_2';\alpha_2\alpha_1}[\delta_{\alpha_1,\alpha_2}\dot{\Pi}_l(q_1 - q_2', \mathrm{i}\epsilon_1 - \mathrm{i}\epsilon_2') + \delta_{\alpha_1,-\alpha_2}\dot{\chi}_l(q_1 + q_2', \mathrm{i}\epsilon_1 - \mathrm{i}\epsilon_2')]\}. \end{aligned}\tag{B.3}$$

Here

$$\dot{\chi}_l(q, \mathrm{i}\epsilon) = \Theta(\mathrm{e}^l - 1 > |q|)\frac{\tilde{v}_l(2 + |q|)}{\epsilon^2 + \tilde{v}_l^2(2 + |q|)^2}, \tag{B.4}$$

$$\dot{\Pi}_l(q, \mathrm{i}\epsilon) = \Theta(\mathrm{e}^l + 1 > |q| > 2)\frac{s_q}{\mathrm{i}\epsilon + \tilde{v}_l q}, \tag{B.5}$$

with $s_q = \mathrm{sign}(q)$. Setting external momenta and frequencies equal to zero we obtain from equation (B.3)

$$\dot{\Gamma}_l^{(4)}(\alpha_1', 0, \alpha_2', 0; \alpha_2, 0, \alpha_1, 0) = -\tilde{g}_l^2 A_{\alpha_1'\alpha_2';\alpha_2\alpha_1}\{\delta_{\alpha_1,\alpha_2}\dot{\chi}_l(0, \mathrm{i}0) - \delta_{\alpha_1,\alpha_2}\dot{\Pi}_l(0, \mathrm{i}0)\} = 0. \quad \text{(B.6)}$$

Inserting this result in equation (2.27) for vanishing momenta and frequencies and using the fact that $\eta = \mathcal{O}(\tilde{g}_l^2)$ this immediately leads to the vanishing of the β-function at one-loop level (equation (3.7)).

Now, for the two-loop flow of the two-point vertex we need the full momentum and frequency dependence of the four-point vertex at the one-loop level. This amounts to calculating the susceptibilities, which are related to the auxiliary functions $\dot{\chi}_l$ and $\dot{\Pi}_l$ via

$$\chi_l(q, \mathrm{i}\epsilon) = \int_0^l \mathrm{d}t\, [\dot{\chi}_{l-t}(\mathrm{e}^{-t}q, \mathrm{e}^{-t}\mathrm{i}\epsilon) - \dot{\chi}_{l-t}(0, \mathrm{i}0)] \quad \text{(B.7)}$$

and

$$\Pi_l(q, \mathrm{i}\epsilon) = \int_0^l \mathrm{d}t\, [\dot{\Pi}_{l-t}(\mathrm{e}^{-t}q, \mathrm{e}^{-t}\mathrm{i}\epsilon) - \dot{\Pi}_{l-t}(0, \mathrm{i}0)]. \quad \text{(B.8)}$$

Performing the integrations we find the results given in equations (3.10) and (3.11).

Finally, we need to express the subtracted four-point vertex, defined in equation (A.3), in terms of the susceptibilities. Up to order $\tilde{g}_l^2$ we obtain from equations (2.29) and (B.3)

$$\begin{aligned}\tilde{\Gamma}_l^{(4,sub)}(Q_1', Q_2'; Q_2, Q_1) \approx \tilde{\Gamma}_{l=0}^{(4,sub)}(Q_1', Q_2'; Q_2, Q_1) - \tilde{g}_l^2\{&A_{\alpha_1'\alpha_2';\alpha_2\alpha_1}\chi_l(q_1 - q_2, \mathrm{i}\epsilon_1 + \mathrm{i}\epsilon_2) \\ &+ E_{\alpha_1'\alpha_2';\alpha_2\alpha_1}[\delta_{\alpha_1,\alpha_2}\Pi_l(q_1 - q_1', \mathrm{i}\epsilon_1 - \mathrm{i}\epsilon_1') + \delta_{\alpha_1,-\alpha_2}\chi_l(q_1 + q_1', \mathrm{i}\epsilon_1 - \mathrm{i}\epsilon_1')] \\ &- D_{\alpha_1'\alpha_2';\alpha_2\alpha_1}\big[\delta_{\alpha_1,\alpha_2}\Pi_l(q_1 - q_2', \mathrm{i}\epsilon_1 - \mathrm{i}\epsilon_2') + \delta_{\alpha_1,-\alpha_2}\chi_l(q_1 + q_2', \mathrm{i}\epsilon_1 - \mathrm{i}\epsilon_2')\big]\}.\end{aligned} \quad \text{(B.9)}$$

Appendix C. Two-loop calculation of the subtracted two-point vertex

In this appendix we give some intermediate results related to section 3.2 concerning the subtracted two-point vertex.

First of all we display the explicit expressions for the inhomogeneities $\dot{\Gamma}_l^{(2,\mathrm{ZS})}$ and $\dot{\Gamma}_l^{(2,\mathrm{PB})}$ obtained in the limit $\Lambda_0 \to \infty$, which amounts to introducing the Dirac sea. This is equivalent to taking $l \to \infty$ in equations (3.13) and (3.14), leading to

$$\begin{aligned}\dot{\Gamma}_\infty^{(2,\mathrm{ZS})}(q, \mathrm{i}\epsilon) &= -\Theta(|q| > 1)2\eta s_q \frac{|q| - 1}{\tilde{v}_0(2 + |q|) + \mathrm{i}\epsilon s_q} \\ &= \Theta(|q| > 1)\eta s_q\left[1 - \frac{3\tilde{v}_0|q| + \mathrm{i}\epsilon s_q}{\tilde{v}_0(2 + |q|) + \mathrm{i}\epsilon s_q}\right],\end{aligned} \quad \text{(C.1)}$$

$$\begin{aligned}\dot{\Gamma}_\infty^{(2,\mathrm{PB})}(q, \mathrm{i}\epsilon) = 2\eta s_q\{&\Theta(|q| > 1)\ln[\tilde{v}_0(2 + |q|) + \mathrm{i}\epsilon s_q] \\ &+ \Theta(1 > |q|)\ln[\tilde{v}_0(4 - |q|) + \mathrm{i}\epsilon s_q] - \ln[\tilde{v}_0(4 + |q|) - \mathrm{i}\epsilon s_q]\}.\end{aligned} \quad \text{(C.2)}$$

The corresponding subtracted function $\dot{\Gamma}_\infty^{(2,sub)}(Q)$ defined in equation (A.4) is in this approximation given by

$$\begin{aligned}\dot{\Gamma}_\infty^{(2,sub)}(q, \mathrm{i}\epsilon) = \eta s_q\Big\{&2\Theta(|q| > 1)\ln[\tilde{v}_0(2 + |q|) + \mathrm{i}\epsilon s_q] \\ &+ 2\Theta(1 > |q|)\ln[\tilde{v}_0(4 - |q|) + \mathrm{i}\epsilon s_q] - 2\ln[\tilde{v}_0(4 + |q|) - \mathrm{i}\epsilon s_q] \\ &+ \Theta(|q| > 1)\left[1 - \frac{3\tilde{v}_0|q| + \mathrm{i}\epsilon s_q}{\tilde{v}_0(2 + |q|) + \mathrm{i}\epsilon s_q}\right] - (\mathrm{i}\epsilon s_q - \tilde{v}_0|q|)\Big\}.\end{aligned} \quad \text{(C.3)}$$

Finally, we show the results obtained by analytic continuation of the subtracted two-point vertex. This is achieved by the replacement $i\epsilon \to \epsilon + i0$ in equation (3.29), and by using the integral representation of the complex function $F(z)$ defined in equation (3.30). It is then easy to verify that

$$\mathrm{Im}\, F(x \pm i0) = \pm\pi\Theta(x > 1)x^{-\eta}. \tag{C.4}$$

In the scaling limit (3.24) and assuming that $|\epsilon^2 - \tilde{v}^2q^2| \gg 1$, we obtain

$$\begin{aligned}\mathrm{Im}\,\tilde{\Gamma}^{(2,sub)}_{\infty}(q, \epsilon + i0) = 2\pi\eta\Bigg\{&\Theta(\epsilon s_q > \tilde{v}|q|)\left|\frac{\epsilon - \tilde{v}q}{4\tilde{v}}\right|^{1-\eta} \\ &+ \Theta(-\tilde{v}|q| > \epsilon s_q > -3\tilde{v}|q|)\left|\frac{\epsilon - \tilde{v}q}{4\tilde{v}}\right|\left|\frac{\epsilon + \tilde{v}q}{2\tilde{v}}\right|^{-\eta} \\ &+ \Theta(-3\tilde{v}|q| > \epsilon s_q)\left|\frac{\epsilon - \tilde{v}q}{4\tilde{v}}\right|^{1-\eta}\Bigg\}.\end{aligned} \tag{C.5}$$

Mathematically the imaginary part of $\tilde{\Gamma}^{(2,sub)}_{\infty}(q, \epsilon + i0)$ arises from the branch cut of $F(x + iy)$ on the real axis for $x > 1$. Furthermore, using the fact that for $|\arg(-z)| < \pi$

$$F(z) = \frac{\pi(1+\eta)}{\sin(\pi\eta)}(-z)^{-\eta} - \frac{1+\eta}{\eta}\,{}_2F_1\left(1, -\eta, 1-\eta; \frac{1}{z}\right), \tag{C.6}$$

we obtain in the regime $|\epsilon^2 - \tilde{v}^2q^2| \gg 1$ and $\eta \ll 1$ for the real part,

$$\begin{aligned}\mathrm{Re}\,\tilde{\Gamma}^{(2,sub)}_{\infty}(q, \epsilon + i0) = &-(\epsilon - \tilde{v}q) + \Theta(\epsilon s_q > -3\tilde{v}|q|) \\ &\times (\epsilon - \tilde{v}q)\frac{1}{2}\left[\left|\frac{\epsilon - \tilde{v}q}{4\tilde{v}}\right|^{-\eta} + \left|\frac{\epsilon + \tilde{v}q}{2\tilde{v}}\right|^{-\eta}\right] \\ &+ \Theta(-3\tilde{v}|q| > \epsilon s_q)(\epsilon - \tilde{v}q)\left|\frac{\epsilon - \tilde{v}q}{4\tilde{v}}\right|^{-\eta}.\end{aligned} \tag{C.7}$$

In deriving equation (C.7), we have neglected corrections of the order of η to the prefactor. Note that the imaginary part given in equation (C.5) is proportional to η, while no such small prefactor appears in the real part, equation (C.7).

References

[1] Sólyom J 1979 *Adv. Phys.* **28** 201
[2] Wilson K G 1972 *Phys. Rev. Lett.* **26** 548
Wilson K G and Kogut J G 1974 *Phys. Rep.* C **12** 75
[3] Ma S K 1976 *Modern Theory of Critical Phenomena* (Reading, MA: Benjamin-Cummings)
[4] Shankar R 1994 *Rev. Mod. Phys.* **66** 129
[5] Fisher M E 1998 *Rev. Mod. Phys.* **70** 653
[6] Emery V J 1979 *Highly Conducting One-Dimensional Solids* ed J T Devreese, R P Evrard and V E van Doren (New York: Plenum)
[7] Voit J 1995 *Rep. Prog. Phys.* **58** 977
[8] Luther A and Peschel I 1974 *Phys. Rev.* B **9** 2911
[9] Meden V and Schönhammer K 1992 *Phys. Rev.* B **46** 15 753
[10] Voit J 1993 *Phys. Rev.* B **47** 6740
[11] Meden V 1999 *Phys. Rev.* B **60** 4571
Meden V 1996 *PhD Thesis* Universität Göttingen
[12] Haldane F D M 1981 *J. Phys. C: Solid State Phys.* **14** 2585
[13] Halperin B I and Hohenberg P C 1969 *Phys. Rev.* **177** 952
[14] Sachdev S 1999 *Quantum Phase Transitions* (Cambridge: Cambridge University Press)
[15] Orgad D 2001 *Phil. Mag.* B **81** 375
Orgad D, Kivelson S A, Carlson E W, Emery V J, Zhou X J and Shen Z X 2001 *Phys. Rev. Lett.* **86** 4362

Carlson E W, Orgad D, Kivelson S A and Emery V J 2000 *Phys. Rev.* B **62** 3422
[16] Ferraz A 2001 *Preprint* cond-mat/0104576
[17] Wegner F J and Houghton A 1973 *Phys. Rev.* A **8** 401
[18] Polchinski J 1984 *Nucl. Phys.* B **231** 269
[19] Nicoll J F, Chang T S and Stanley H E 1976 *Phys. Lett.* A **57** 7
Nicoll J F and Chang T S 1977 *Phys. Lett.* A **62** 287
Chang T S, Vvedensky D D and Nicoll J F 1992 *Phys. Rep.* **217** 279
[20] Wetterich C 1993 *Phys. Lett.* B **301** 90
[21] Morris T R 1994 *Int. J. Mod. Phys.* A **9** 2411
[22] Wegner F 1994 *Ann. Phys., Lpz.* **3** 77
[23] Zanchi D and Schulz H J 1996 *Phys. Rev.* B **54** 9509
Zanchi D and Schulz H J 1997 *Z. Phys.* B **103** 339
Zanchi D and Schulz H J 2000 *Phys. Rev.* B **61** 13 609
[24] Salmhofer M 1998 *Renormalization* (Berlin: Springer)
Honerkamp C, Salmhofer M, Furukawa N and Rice T M 2001 *Phys. Rev.* B **63** 45 114
Salmhofer M and Honerkamp C 2001 *Prog. Theor. Phys.* **105** 1
Binz B, Baeriswyl D and Douçot B 2002 *Eur. Phys. J.* B **25** 69
Honerkamp C 2000 *PhD Thesis* ETH Zürich
[25] Kehrein S 1999 *Phys. Rev. Lett.* **83** 4914
Heidbrink C P and Uhrig G S 2002 *Phys. Rev. Lett.* **88** 146401
[26] Halboth C J and Metzner W 2000 *Phys. Rev.* B **61** 4364
Halboth C J and Metzner W 2001 *Phys. Rev. Lett.* **85** 5162
Halboth C J 1999 *PhD Thesis* (Aachen: Shaker)
[27] Kopietz P and Busche T 2001 *Phys. Rev.* B **64** 155101
[28] Blagoev K B and Bedell K S 1997 *Phys. Rev. Lett.* **79** 1106
Yamanaka M, Oshikawa M and Affleck I 1997 *Phys. Rev. Lett.* **79** 1110
[29] Schulz H J and Shastry B S 1998 *Phys. Rev. Lett.* **80** 1924
[30] Luttinger J M 1960 *Phys. Rev.* **119** 1153
[31] Kopietz P 2001 *Nucl. Phys.* B **595** 493
[32] Metzner W and Di Castro C 1993 *Phys. Rev.* B **47** 16 107
[33] Arrigoni E 1999 *Phys. Rev. Lett.* **83** 128
[34] Busche T and Kopietz P unpublished
[35] See for example
Lifshitz E M and Pitaevskii L P 1980 *Statistische Physik, Teil 2* (Berlin: Akademie) p 72
[36] Ivanchenko Y M and Lisyansky A A 1995 *Physics of Critical Fluctuations* (New York: Springer)